Research article

Journal of Atoms and Molecules
An International Online Journal
ISSN–2277 –1247

CODEN (USA) CODE: JAMOF4

Calculation of structure, phonon vibrational spectra, thermodynamic properties and superconductivity of calcium dinitride by First-principles

L.Q. Zhang, J. F. Zhang, F. S. Mu, G. L. Zong, S. T. Xu*

Information College, Huaibei Normal University, Huaibei 235000, China

Received on: 14-09-2018 Revised on: 16-10-2018 Accepted on: 28-10-2018

ABSTRACT

A first-principles investigation of the crystal structure, stability, and electron-phonon interactions of calcium dinitride (CaN_2) is described, and CaN_2 is predicted to be a superconducting material. By using the Debye-Grüneisen model, the thermodynamic properties of CaN_2, including the Debye temperature Θ_D, the thermal expansion coefficient α and the Grüneisen parameter γ, are successfully obtained in the temperature range from 0 to 3000 K and the pressure range from 0 to 500 GPa. The phonon mode frequencies at Γ and the total and partial phonon densities of states for CaN_2 are discussed in detail. The dispersion curves of CaN_2 show large pseudo-gaps in the 400–1300 cm^{-1} range. The total of the electron-phonon coupling constants for CaN_2 is given by $\lambda = 0.37$, with a corresponding estimated superconducting temperature of $Tc \approx 1\ K$. The estimated superconducting temperature of CaN_2 rose to 28.8 K as the pressure increased to 10 GPa, and then decreased monotonically at higher pressures to almost zero at 50 GPa.

KEY WORDS: electron-phonon interaction; superconducting temperature; phonon density of states; Eliashberg spectral function

*** Corresponding author**

S. T. Xu
Email: stxu@imr.ac.cn

INTRODUCTION

Binary metal nitrides containing dinitrogen anions $[N_2]^{2-}$ with N=N double bonds have attracted increasing attention in both experimental and theoretical investigations [1-7]. In 2001, SrN_2 and BaN_2 were synthesized at 893 K and at 0.55–0.56 GPa for the first time. [1-7] From then on, a number of binary metal nitrides with high hardness, high superconductivity, photoluminescence and antiferromagnetic and ferromagnetic properties attracted extensive attention in the materials science field [3-7].

Yong *et al.* synthesized OsN_2 and IrN_2 at higher process pressures and temperatures.[8] They found that IrN_2 is a superhard material with low compressibility and of a very high bulk modulus B=428 GPa. Crowhurst *et al.* found that platinum nitride has high strength and greater durability.[9] The discovery of superconductivity in MgB_2 (with a higher superconducting transition temperature T_c=39 K) has led to extensive theoretical and experimental studies for this metal nitrides [10-12]. Alexander *et al.* predicted theoretically that OsN_2 is a superconducting material with an estimated superconducting temperature T_c≈1 K, and after hole doping, [13] the superconducting temperature T_c increases to 4 K.

In this work, we will investigate three possible CaN_2 structures, including the isostructural to marcasite structure, the tetragonally distorted NaCl structure, and the tetragonally distorted structure, by first-principles calculations. It is found that the tetragonally distorted NaCl structure is more stable at low pressure than other crystal phases that have been synthesized experimentally up to now. In addition, we study the phonon dispersion, thermodynamic properties and superconductivity of CaN_2 with the tetragonally distorted NaCl structure in detail.

THEORETICAL METHOD AND COMPUTATION DETAILS

Total energy electronic structure calculations

We used the plane-wave pseudopotential density functional theory method as implemented in the Cambridge serial total energy package (CASTEP) for the lattice parameter optimization [14]. The generalized gradient approximation (GGA) proposed by Perdes *et al.* in the Perdew-Burke-Ernzerhof scheme to describe the exchange and correlation potentials [15]. The phonon dispersions were obtained in the linear response via density functional theory (DFT) with the Quantum-ESPRESSO program, [16] where the ion-electron interaction are represented by ultrasoft pseudopotentials for N and Ca atoms, and the N $2s^2 2p^3$ and Ca $3p^6 4s^2$ electrons are explicitly treated as valence electrons [17]. The generalized gradient approximation (GGA) of Perdew-Burke-Ernzerhof was adopted for the exchange-correlation potentials, with cutoffs of 90 Ry for the wave functions and 900 Ry for the change density [18].

The dynamical matrices and the electron phonon coupling constants λ were calculated using density functional perturbation theory (DFPT) in the linear response regime [19]. The electronic Brillouin zone (BZ) integration in the phonon calculation was performed over a 24×24×24 k-point mesh. The electron-phonon coupling was found to be converged with a finer grid of 18×18×18 k points and a Gaussian smearing of 0.004 Ry. Dynamical matrices was calculated on a 3×3×3 mesh of phonon wave vectors q. The phonon dispersion was then obtained on a finer 9×9×9 $\boldsymbol{q}$ mesh by Fourier interpolation of the real space interatomic force constants. In this way, λ is calculated over a 9×9×9 $\boldsymbol{q}$ point mesh. The convergence of total energy calculations with respect to the number of k-points and the cut-off energy is well checked.

Thermodynamic properties

Thermodynamic properties are very important in understanding the thermal response of the solids. We here apply the quasi-harmonic approximation (QHA) to study the thermodynamic properties of the I4/mmm structure of CaN_2 [20, 21]. In the QHA model, the non-equilibrium Gibbs function

$G^*(V,p,T)$ under a given pressure p and temperature *T* takes the form of

$$G^*(V,p,T) = E_{sta}(V) + pV + F^*_{vib}(V,T) \quad (1)$$

where the static energy E_{sta} is the direct result of the electronic structure calculation, the vibrational contribution to the Helmholtz energy is given by

$$F^*_{vib} = \int_0^\infty \left[\frac{\hbar\omega}{2} + k_B T \ln\left(1 - e^{-\hbar\omega/k_B T}\right) \right] g(\omega,x) d\omega \quad (2)$$

where $g(\omega,x)$ is the phonon density of state, which depends on the crystal geometry. The equilibrium entropy (*S*), Helmholtz free energy (*F*), Gibbs free energy (*G*), internal energy (*U*), constant-volume heat capacity (C_V), and isothermal bulk modulus (B_T) are then expressed as

$$S = S\left(V(p,T),T\right) = \sum_j \left[-k_B \ln\left(1 - e^{-\omega_j/k_B T}\right) + \frac{\omega_j}{T} \frac{1}{e^{\omega_j/k_B T} - 1} \right] \quad (3)$$

$$C_V = C_V\left(V(p,T),T\right) = \sum_j k_B \left(\frac{\omega_j}{k_B T} \right)^2 \frac{e^{-\omega_j/k_B T}}{\left(e^{-\omega_j/k_B T} - 1\right)^2} \quad (4)$$

$$B_T = -V\left(\frac{\partial p}{\partial V}\right)_T = V\left(\frac{\partial^2 F}{\partial V^2}\right)_T \quad (5)$$

The volume derivative of $-TS$ used to compute Grüneisen ratio γ_{th}

$$\gamma_{th} = -\frac{V}{C_v T}\left(\frac{\partial(-TS)}{\partial V}\right)_T \quad (6)$$

The thermal expansion codfficient (α), constant-heat capacity (C_p), and adiabatic bulk modulus (B_s) are given as follows

$$\alpha = -\frac{1}{V}\left(\frac{\partial V}{\partial T}\right)_p = \frac{\gamma_{th} C_v}{V B_T} \quad (7)$$

$$C_p = \left(\frac{\partial H}{\partial T}\right)_p = C_v(1 + \gamma_{th}\alpha T) \quad (8)$$

$$B_S = -V\left(\frac{\partial p}{\partial V}\right)_S = V\left(\frac{\partial^2 U}{\partial V^2}\right)_S = B_T(1 + \gamma_{th}\alpha T) \quad (9)$$

Phonon dispersion

The harmonic approximation is usually a typical description for the physics of phonon, in which the equation of motion takes the form of [22]

$$\omega^2(k,l)e(k,l) = D(k)e(k,l), \quad (10)$$

where $\omega(k,l)$ is the phonon frequencies, $e(k,l)$ describing the corresponding atomic displacement, $D(k)$ is the dynamic matrix, which can be obtained from the force constant matrix Θ

$$D_{st}^{\alpha\beta}(k) = \frac{1}{\sqrt{M_t M_s}} \sum_R \Theta_{st}^{\alpha\beta}(R) \exp(-ik \cdot R), \quad (11)$$

where M_s and M_t are masses for atoms *s* and *t*, respectively, *R* is the Bravais lattice vectors. With the frame work of harmonic approximation, keeping only the second terms in the Taylor series of total energy *E*, Θ is given by

$$\Theta_{st}^{\alpha\beta} = \frac{\partial^2 E}{\partial \mu_s^\beta \partial \mu_t^\beta}, \quad (12)$$

where μ_s^α is the displacement for atom s from its equilibrium position in α direction. Consequently the force f exerted on atom s relating the displacement of atom t is

$$f_s = -\Theta_{st}\mu_t. \quad (13)$$

We perform the supercell method to determine the dynamical matrix from Eq. (11), [23] in which the forces are calculated with respect to the atoms perturbed from their equilibrium positions and frozen in.

Superconductivity

In the density-functional perturbation theory (DFPT) calculations, [19] the electron-phonon interation for a phonon mode ν with momentum $\boldsymbol{q}$ can be calculated as

$$\lambda_{q\nu} = \frac{4}{\omega_{q\nu} N(E_F) N_k} \sum_{k,n,m} \left| g_{kn,k+qm}^{\nu} \right|^2 \delta(\in_{kn}) \delta(\in_{k+qm}) \quad (14)$$

where the sum is over the Brillouin zone. The matrix element is $g_{kn,k+qm}^{\nu} = \langle kn \left| \delta V / \delta u_{q\nu} \right| k+qm \rangle \Big/ \sqrt{2\omega_{q\nu}}$, where $u_{q\nu}$ is the amplitude of the displacement of the phonon and V is the Kohn-Sham potential. The electrom-phonon coupling is calculated as a BZ average over the phonon wave vectors $\lambda = \sum_{q\nu} \lambda_{q\nu} / N_q$. The Eliashberg spectral function depends directly on the electron-phonon matrix element:

$$\alpha^2 F(\omega) = \frac{1}{N(E_F) N_k} \sum_{kq\nu} \left| g_{nk,m(k+q)}^{\nu} \right|^2 \times \delta(\varepsilon_{nk}) \delta(\varepsilon_{m(k+q)}) \delta(\omega - q\nu) \quad (15)$$

Here, N_k is the number of k-points used in the summation, $N(E_F)$ is the DOS at the Fermi level, and $\omega_{q\nu}$ denotes the phonon frequencies. The electron–phonon matrix element $\left| g_{nk,m(k+q)}^{\nu} \right|^2$ is defined by the variation in the self-consistent crystal potential.

RESULTS AND DISCUSSION

Structural properties and stability of CaN_2

Wessel *et al.* investigated 15 possible structures of CaN_2 and found that the possible ground state structure belonged to the space group $pnaz_1$,[24] with a=7.49 Å, b=6.275 Å and c=4.574 Å, and Ca1 in (4a), N1 in (4a) and N2 in (4a). However, the experimental results measured by powder X-ray diffraction showed that CaN_2 crystallizes in a tetragonally-distorted NaCl-type structure with space group *I4/mmm*. [25] The electronic structure of CaN_2 indicated that the compound had metallic properties [25].

We relaxed 15 different well-known AB_2 structure types by simultaneously varying the cell volume and the cell parameters without applying any constraints to examine new structural candidates [1,24]. It is found that the marcasite structure, the tetragonally distorted NaCl-type structure and the more distorted tetragonal structure are the possible three structures considered. The three structures have similar energy within the variation of 10meV/CaN_2, which means a rather flat energy landscape near the energy minama.

In the marcasite structure (space group Pmmm), the calcium atoms are in the Wyckoff 2a sites and nitrogen atoms in the 4g sites. In the tetragonally distorted NaCl-type structure (space group I4/mmm), the calcium atoms are in the Wyckoff 2a sites and nitrogen atoms in the 2b sites. In the case of a more distorted tetragonal structure (space group C2/c), the calcium atoms are in the Wyckoff 8f sites and nitrogen atoms in the 4e sites. However, Wessel and Dronskowski *et al.* had speculated on theoretically that CaN_2 belong to space group $Pna2_1$ and then we could not find the similar structure in this work [26].

In Fig. 1, we present the *E-V* curves for the three possible structures. Fig. 1(a) indicates that CaN_2 undergoes a transition from I4/mmm phase to Pmmm phase when the pressure is 3 GPa, and Fig. 1(b) shows that there is a transition from the marcasite and tetragonally distorted NaCl structures to the more tetragonally distorted structure CaN_2 at 14 GPa. Wang *et al.* declared that oP12 structure (face centered cubic structure with Pnma space group) would complete a phase transition to tI6 (I4/mmm phase) at 2.9 GPa and change to the more tetragonally distorted structure when pressure is higher than 12 GPa [27]. Our results are consistent with these results. Unfortunately, this structure has not been confirmed experimentally up to date due to the experimental difficulties. In Table 1, we list the calculated equilibrium volume (V_0), the equilibrium lattice parameters, the bulk modulus (B_0) by fitting the total energies as a function of volume to the Vinet equation of state (EOS) and the distance of N-N, [28] together with other previously reported theoretical and experimental data [25, 27, 29]. The equilibrium unit cell volumes are 38.34 $Å^3$ are higher than the experimental value 38.24 $Å^3$ with the errors of 0.2% [25]. Our results are excellent agreement with the experimental and other theoretical data [25, 27, 29].

The experimental results measured by powder X-ray diffraction showed that CaN_2 crystallizes with space group *I4/mmm* at room temperature and zero pressure, [25] with a=3.575 Å, c=5.984 Å, V=76.472 $Å^3$ and Z=2, and Ca1 in (2a) and N1 in (4e). Recently, by using unbiased structure searching method, Wang *et al.* investigated the energy landscape of CaN_2 and declared that when the pressure is above 2.9 GPa the tetragonally distorted NaCl structure phase of CaN_2 would become the thermodynamic ground state [27].

Table 1 Equilibrium properties of the tetragonally distorted NaCl structure-type phase of CaN_2.

	V_0 (Å^3)	a (Å)	c (Å)	B_0 (GPa)	B_0'	N-N (Å)
GGA (Present)	38.34	3.607	6.097	55.81	4.21	1.236
Calculated data [a]	38.83	3.604	5.978			1.257
Calculated data [b]	39.41	3.620	6.010			1.258
Exp. [c]	38.24	3.575	5.984			1.202

[a] Obtained from unbiased structure searching method by Wang *et al.*; [27]

[b] Obtained from GGA-PBE-PAW method (VASP) by Kulkarni *et al.*; [29]

[c] From the powder X-ray diffraction by Schneider *et al* [25].

Phonon dispersion

The calculated phonon dispersions of CaN_2 at 0 GPa for Pmmn phase, 5, 10 GPa for I4/mmm phase and 12 GPa for C2/c phase are plotted in Fig. 2. The tetragonal phase of CaN_2 (I4/mmm phase) shows D_{4d} point group symmetry. Based on the lattice structure and this symmetry, the numbers of the Raman and infrared active modes can be predicted using group theory.[30] For the three atoms per primitive cell in the CaN_2 case, there are nine vibrational modes at the Γ-point of the Brillouin zero and at the nine phonon point bands extending up to 1600 cm^{-1}. The zone center optical phonon modes are decomposed according to the following representation: D_{4d}: $4Bu \oplus 2Au \oplus 2Ag \oplus Bg$. The three acoustic modes with zero frequencies at the Γ-point can be identified as the *Bu*(LA) and *Au*(TA) modes, [31] where *Bu* and *Au* are both translations. LA denotes the longitudinal acoustic branch, while TA denotes the transverse acoustic branch. The six optical branches are identified as *Bu*, *Ag*, *Bg*, and *Au* modes. The *Bu* and *Au* modes are Raman active modes, while the *Ag* and *Bg* modes are infrared active modes (including infrared absorption or reflection). Fig. 2 (a) clearly shows that the entire BZ under pressure of 0 GPa for Pmmn phase is dynamical stability because of the absence of any imaginary frequency modes. However, the volume of the Pmmm phase collapse by 1.19% ($\triangle$ V=0.21Å^3/CaN_2) in the vicinity of 3 GPa and mechanically unstable while pressure elevated to 3 GPa for imaginary frequency modes. From these results, the Pmmm phase is mechanically stable structure at standard and slightly elevated pressure. At about 3 GPa, the Pmmm phase transforms into the I4/mmm phase type. The Pmmm phase is the mechanical ground state of CaN_2. Recently, Wang *et al* had predicted that the thermodynamic ground state of CaN_2 was oP12 structure (Pamn space group) and would undergo a first-order phase transition to tI6 structure (I4/mmm space group) at about 2.9 GPa [27]. The results are similar with our conclusion. The phonon dispersion curves for CaN_2 in Fig. 2 (a) show that the phonon branches are distributed almost uniformly up to 400 cm^{-1} in all high symmetry directions. In the CaN_2 case, we found a large pseudogap between 400 and 1300 cm^{-1}. Sanjay et al. predicted that the high frequencies mainly contribute to the vibrations of the N=N bond in dimers, and that the lower frequency comes from the vibrations of the metal element [32]. The phonon dispersions curve for I4/mmm phase of CaN_2 under 5 to 10 GPa pressure range are given in Fig. 2 (b) and (c), and

found that frequency stabilization occurred even when the pressure increased to 10 GPa and the large pseudo gap was still there. Meanwhile, the I4/mmm phase is dynamical stability with the increased pressure for the absence of any imaginary frequency modes.

Furthermore, we investigate the phonon dispersions relation of I4/mmm phase through increased pressure and find the imaginary frequencies when pressure higher up to 13 GPa. The conclusion is consistent with Schneider *et al* who successfully synthesized CaN_2 in laboratory at 12 GPa in a multianvil pressure, [25] which means the I4/mmm phase is mechanically stable at 12 GPa. When the pressure close to 14 GPa, one of the acoustic modes changed into imaginary frequency modes, which means that the structures are unstable, as shown in Fig. 3 for I4/mmm phase. We further investigated the phonon dispersion curves of C2/c phase at 14 and 20 GPa, and found the mechanically unstable, which means the model of C2/c phase is not exist. Then, the frequency difference of the large pseudogap transformed from 700 to 1500 cm^{-1} is shown in Fig. 3, which means that the phonon dispersion curves moved towards the higher frequency. Chen et al. obtained similar results when they predicted that PdN_2 would dissociate under pressure as it increased to 18 GPa [33]. Naturally, further studies of this behavior in the future will require far more laboratory testing.

In Table 2, we listed the phonon mode frequencies at Γ for Pmmm phase at 0 GPa, 3, 10, 12, 13 GPa for I4/mmm phase, 20 GPa for C2/c phase, which changed with increasing pressure. It is clearly shown that the phonon modes *Bu1* and *Bu2* shift to lower frequencies as the pressure increases. However, the *Au1*, *Bu3*, *Ag1*, *Bu4*, *Bg* and *Au2* phonon modes decreased with increasing pressure up to 10 GPa, and then increased monotonically with increasing pressure. Our calculated values of the corresponding phonon density of states ($G(\omega)$) and Eliashberg spectral function $\alpha^2 G(\omega)$ of CaN_2 for pressures up to 20 GPa are shown in Fig. 4. Increases in the electron-phonon coupling strength in Pmmm, I4/mmm, C2/c phase of CaN_2 with increasing pressure can be clearly observed in Fig.4. At the same time, the peak moves towards the lower energy region with increasing pressure.

Table 2 Phonon mode frequencies (cm^{-1}) at Γ at different pressure *P* (GPa). I: infrared active, R: Raman active

P	Bu_1(I)	Bu_2 (I)	Au_1(I)	Bu_3(I)	Ag_1(R)	Bu_4(I)	*Bg*(I)	Au_2(I)	Ag_2(R)
0	0	23.4	24.4	225.9	338.9	354.2	525.5	532.9	1647.9
3	4.5	21.4	23.7	230.1	381.4	386.7	596.5	622.9	1641.1
10	14.4	20.3	23.4	228.3	367.7	378.0	564.2	580.7	1477.7
12	14.4	18.7	22.9	235.5	355.5	366.3	531.5	538.8	1657.9
13	16.0	14.8	20.6	246.2	357.4	370.2	532.4	540.5	1664.5
20	17.6	13.6	14.7	252.0	409.8	425.9	643.4	678.1	1660.8

Thermodynamic properties of CaN_2

Within the framework of the quasi-harmonic approximation, we obtained the pressure and temperature dependences of the thermodynamic properties of the solid phases from quantum-espresso program and produced data for CaN_2.[16] By applying the quasi-harmonic approximation, we obtain the Debye temperature Θ_D, constant-volume heat capacity C_V, the thermal expansion coefficient α, and the Grüneisen parameter γ.

In Fig. 5 we show the curves of constant-volume heat capacity C_V with pressure and temperature in the I4/mmm and Pmmm phase of CaN_2. In Fig. 5, the results show that C_V decreased linearly with the pressure increases at a given temperature. As the pressure goes higher, the discrepancy between C_V at fixed pressure increases gradually at different temperature of T=0 K and 300 K, respectively. However, the various temperatures had hardly any influence on the constant-volume heat capacity C_V when the temperature was exceed 600 K until to 900 K with the pressure increase. We can therefore conclude that the effect of the higher temperature on heat capacity C_V is not as important as lower temperatures. From Fig. 6, we find that at a given temperature, the Debye temperature Θ increases almost linearly with the pressure for both structures. As the temperature goes higher, the discrepancy between Θ at different temperature is hard any influence at a given pressure. The four curves are all most parallel to each other with the pressure increases, which means the vibration frequency of the particles in CaN_2 with the pressures and the temperature have the similar tendency.

Thermal expansivity α is a very important parametric quantity for interpretation of the thermodynamic and thermodynamic behavior of solids at high temperatures. [34] The obtained variation of thermal expansion coefficient α with pressure at different temperature for I4/mmm and pmmm phase of CaN_2 are shown in Fig. 7. Fig. 7 shows thermal expansivity α decreases linearly gradually at different temperatures with the pressure elevates. This means that the effect of pressure on α plays a significant role. These results are in accordance with the results of the capacity heat C_V which apples to many kinds of materials. In Fig. 8, we show the variation of the Grüneisen parameter γ with pressure at different temperature. The Grüneisen constant γ can help us to correctly predict harmonic effects in the vibrating lattice and the effects of temperature on the phonon frequencies and line widths. Fig. 8 shows that γ decreases linearly more quickly as the temperature increases from 0 K to 900 K with the applying of pressure for both structures. At fixed pressures, the discrepancy between γ are very little with the temperature changed from low temperature range 0 K to high temperature range 900 K. This means that the anharmonic properties of CaN_2 have a prominent influence with increasing temperature, from which we can predict that the phonon frequencies and linewidths will change remarkably when the temperature increases at zero pressure.

Superconductivity of CaN_2

Finally, we show the pressure dependence of λ and superconducting temperature T_c for CaN_2 in Fig. 9. We find that λ increases with increasing pressure up to 13 GPa, but a significant discrepancy is found when the pressure increases beyond 13 GPa. We found that λ decreased monotonically from 0.65 at 13 GPa to 0.30 at 20 GPa. Using the Allen-Dynes formula [35, 36]:

$$Tc = \frac{\omega_{\ln}}{1.2}\exp\left[-\frac{1.04(1+\lambda)}{\lambda-\mu^{*}(1+0.62\lambda)}\right] \quad (16)$$

With the Coulomb parameter $\mu^{*}=0.1$, we finally obtain T_c≈4.4 K. We compared our results with the theoretical results of Alexander et al., [13] which declared that the total electron-phonon coupling of OsN_2 was λ=0.37 with an estimated superconducting temperature T_c≈1 K, and when the doping concentration increased to 0.25, T_c increased to 4 K. We found that the T_c of CaN_2 is closer to that of the doped OsN_2. [36] By adopting the conventional value of μ^{*} as 0.1, we solve the McMillan equation to derive T_c at different pressures in Fig. 9. The T_c was found to increase with pressure from 0 to 13 GPa and then decrease monotonically with increasing pressure from 13 to 20 GPa, almost reaching 0 K at 20 GPa. Meanwhile, the structure of CaN_2 becomes unstable and has a transition of structure when the pressure increased up to 13 GPa. The phenomenon is consistent with phonon dispersion curves became imaginary frequency modes when pressure higher up to 13 GPa. Furthermore, when CaN_2 undergoes a transition more lower superconducting temperature owned by the more tetragonally distorted structure.

CONCLUSION

The crystal structure, thermodynamic properties, phonon vibrational spectra and pressure-induced phase transitions of calcium nitride (CaN_2) have been studied extensively using first-principles calculations. By fitting *E-V* curves, we confirmed that the tetragonally distorted NaCl-type structure was mechanically stable at zero temperature and room pressure. Using the quasi-harmonic approximation, the thermodynamic properties of the material, including constant-volume heat capacity C_V, the Debye temperature Θ_D, the thermal expansion coefficient α and the Grüneisen parameter γ, are predicted at high temperatures and zero pressure. The C_V change obviously at lower temperature with a given pressure, and decreases gradually with the pressure increases. These results are in accordance with the results of thermal expansivity α. The discrepancy between Θ at different temperature is hardly any influence at a given pressure as the temperature goes higher. These results are in consistent with the results of Grüneisen parameter γ.

In addition, detailed analysis of the phonon dispersion curves at zero temperature and pressure allowed us to conclude that the phonon dispersion curves contain positive frequencies throughout the entire BZ and confirmed their dynamical stability. When the pressure exceeds 13 GPa, one of the acoustic modes became imaginary frequency modes, which indicates dynamical instability. The superconducting temperature T_c was found to increase with pressure from 0 to 3 GPa for Pmmm and I4/mmm phase and then decrease monotonically with further increases in pressure from 13 to 20 GPa, which is consistent with the acoustic modes becoming imaginary frequency modes when the pressure increased to 13 GPa. We predict that CaN_2 is a superconducting material, and that its superconducting transition temperature increases with increasing pressure up to 28.8 K.

ACKNOWLEDGMENT

The authors would like to thank the National Natural Science Foundation of China (No.51502106 and No. 41705012) and the Natural Science Foundation of Education Committee of Anhui Province (No. KJ2016B003, No.KJ2017A844 and KJ2018A0680) for supporting the work.

REFERENCES

1) Auffermann, G., Prots, Y and Kniep, R. Angew Chem. Int. Ed. 40**,** 547(2001).
2) Vajenine, VG., Auffermann, G., Prots, Y., Schelle, W., Kremer, KR., Simon, A and Kniep, R. Inorg. Chem. 40, 4866 (2001)
3) Auffermann, G., Kniep, R., Bronger, W., Anorg, Z. Allg. Chem. 632, 565 (2006).
4) Yamanaka, S., Hotehama, K., and Kawaji, H. Nature 392, 580 (1998).
5) McMillan, FP. Nature Mater. 1, 19(2002).
6) Maruyama, T., and Morishita, T. Appl. Phys. Lett 69, 890(1996).
7) Zerr, A., Miehe, G., and Boehler, R. Nature Mater. 2, 185 (2003).
8) Young, FA., Sanloup, C., Gregoryanz, E., Scandolo, S., Hemley, JR., and Mao, KH. Phys. Rev. Lett. 96, 155501 (2006).
9) Crowhurst, CJ., Goncharov, F., Sadigh, B., Evans, LC., Morrall, GP., Ferriva, LJ., and Nelson, GA. Science 311, 1275(2006).
10) Nagamatsu, J., Nakagawa, N., Muranaka, T., Zenitani, Y., and Akimitsu, J. Nature 410, 63(2001).
11) Tomita, T., Hamlin, JJ., Schiling, SJ., Hinks, GD and Jorgensen, DJ. Phys. Rev. B 64, 092505 (2001).
12) Wang, CY., Lv, J., Ma, MY., Cui, T and Zou, TG. Phys. Rev. B 80, 092505 (2009).
13) Hernández, AD., Javier, MA., Gianni, P and Sandro, S. Phys. Rev. B 77, 092504 (2008).
14) Segall, DM., Lindan, DJP., Probert, JM., Pickard, JC., Hasnip, JP., Clark, JS., Payne, CM. J. Phys.: Condens. Matt. 14, 2717(2002).
15) Perdew, PJ., Burke, K and Ernzerhof, M. Phys. Rev. Lett. 77, 3865 (1996).
16) Baroni, S., Corso, DA., Gironcoli, S., Giannozzi, P., Cavazzoni, C., Ballabio, G., Scandolo, S., Chiarotti, G., Focher, P., Pasquarello, A., Laasonen, K., Trave, A., Car, R., Marzari, N. and A. Kokalj, A. http://www.quantum-espresso.org.
17) Vanderbilt, D. Phys. Rev. B 41, 7892 (1990).
18) Perdew, PJ., Burke, K and Ernzerhof, M. Phys. Rev. Lett. 77, 3865 (1996).
19) Baroni, S., de. Gironcoli, S., Dal Corso, A and Giannozzi, P. Rev. Mod. Phys. 73, 515 (2001).
20) Born, M and Huang, K. Dynamical Theory of Crystal Lattices (2^{nd} end.) (USA: Oxford University Press) p. 40(1988).
21) Otero-de-la-Roza, A., Abbasi-Pérez, D. and Luaña, V. Comput. Phys. Commun. 182, 2232(2011).
22) Kaxiras, E. Atomic and Electronic Structure of Solids (1^{st} edn.) (New York: Cambridge University Press) p. 22 (2003).
23) Baroni, S., de Gironcoli, S., Dal Corso, A and Giannozzi, P. Rev. Mod. Phys. 73, 515 (2001)
24) Wessel, M and Dronskowski, R. J. Comput. Chem. 31, 1613 (2010).
25) Schneider, BS., Frankovsky, R and Schnick, W. Inorg. Chem. 51, 2366(2012).
26) Michael, W and Richard, D. J. Comput. Chem. 31, 1613 (2010).
27) Wang, H., Yao, SY., Si, LY., Wu, JZ and Vaitheeswaran, G. J. Phys. Chem. C 118, 650 (2014).
28) Vinet, P., Rose, HJ., Ferrante, J and Smith, RJ. J. Phys.: Condens. Matt. 1, 1941 (1989).
29) Kulkarni, A., Schòn, CJ., Doll, K and Jansen, M. Chem. Asian J. 8, 743 (2013).
30) Plymate, GT., and Stout, HJ. J. Geophys, Res. B 94, 9477(1989).
31) Rouseau, LD., Bauman, PR., and Porto, SPS. J. Raman Spectrosc. 10, 253 (1981).

32) Sanjya, GD., Sanjeev, GK. and Prafulla, JK. Eur. Phys. J. B 86, 8(2013).
33) Chen, W., Tse, SJ., Jiang, ZJ. J. Phys.: Condens. Matt. 22, 015404 (2010)
34) Allen, P and Dynes, R. Phys. Rev. B 12, 905 (1975).
35) Mchillan, W. Phys. Rev. 167, 331 (1968).
36) Hernández, DA., Montoya, AJ., Profeta, G. and Scandolo, S. Phys. Rev. B 77, 092504 (2008).

Figures:

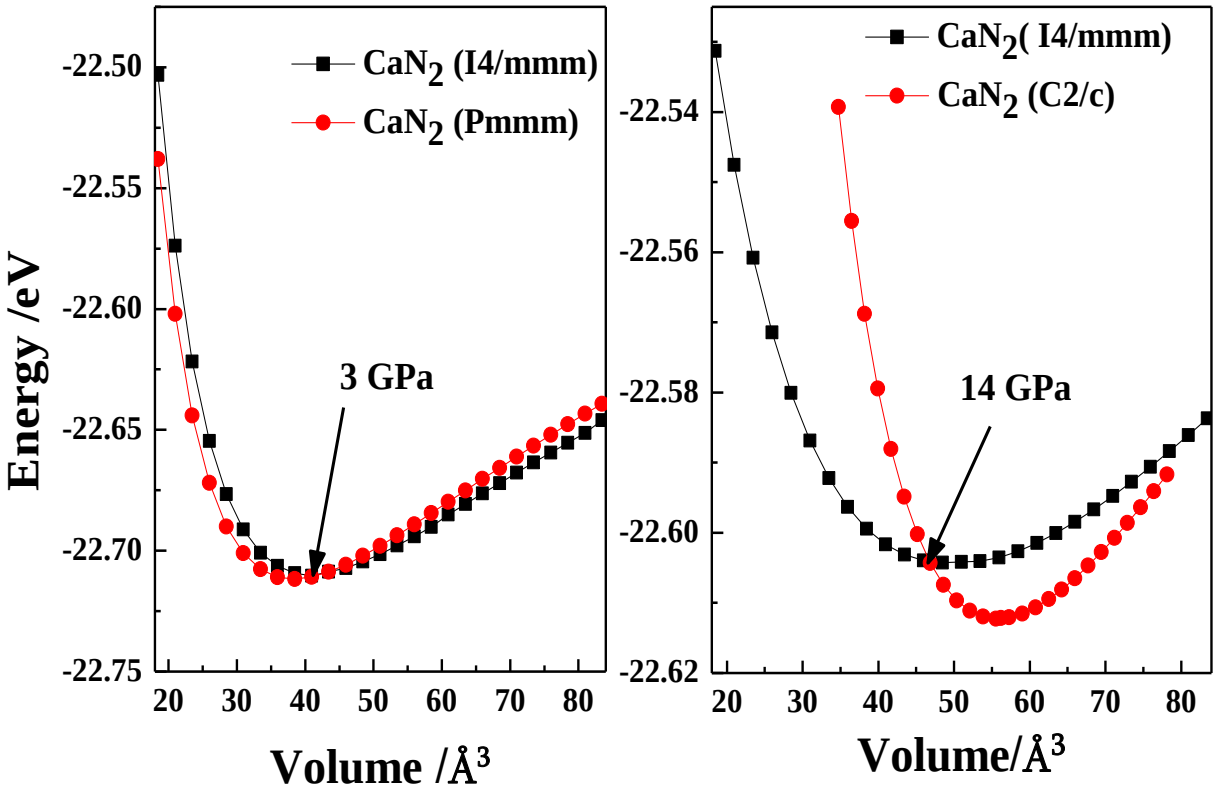

Fig. 1 (a) Energy as a function of the volume per formula unit for marcasite-type (Pmmm) and tetragonally distorted NaCl-type structure (I4/mmm) of CaN_2 and the phase transition from I4/mmm phase to Pmmm at 3 GPa; (b) Energy as a function of the volume per formula unit for a more distorted tetragonally-type structure (C2/c) of CaN_2 and the phase transition from I4/mmm phase to C2/c at 12 GPa.

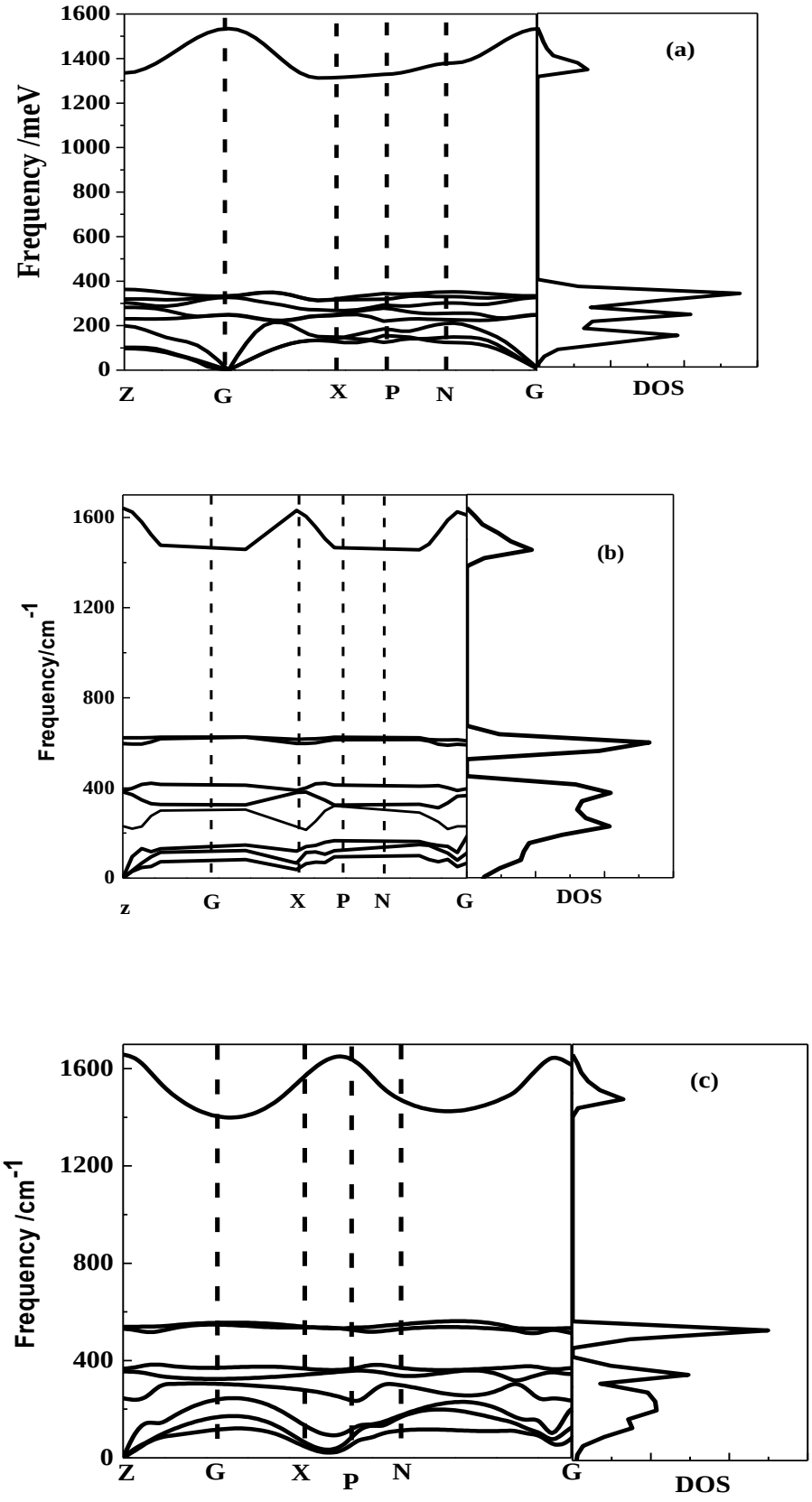

Fig. 2 Calculated phonon dispersion curves of CaN_2 at 0 GPa for Pmmm (a), 5 GPa (b) and 13 GPa for I4/mmm (c). The right panel is the phonon density of state $G(\omega)$.

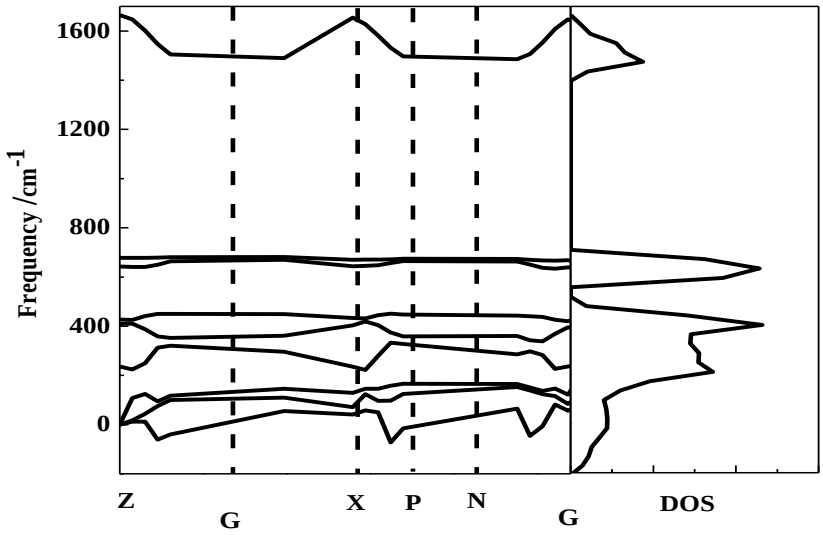

Fig. 3 Calculated phonon dispersion curves of CaN_2 at 14 GPa for I4/mmm. The right panel is the phonon density of states $G(\omega)$

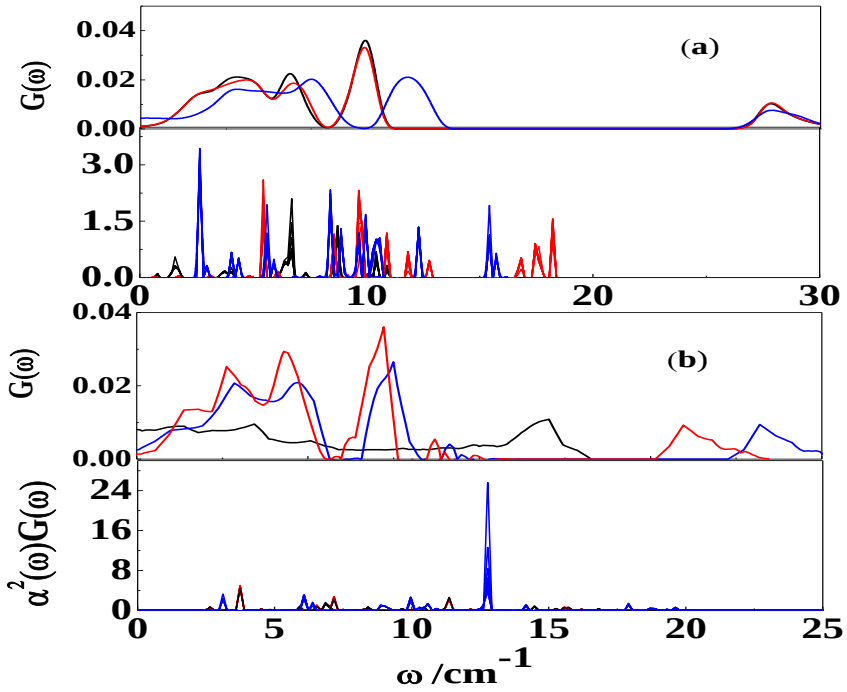

Fig. 4 (color online). The phonon density of states of states $G(\omega)$(1th and 3th panels) and the Elishberg function $\alpha^2 G(\omega)$(2nd and 4th panels) of CaN_2 as a function of pressure. The $G(\omega)$ and $\alpha^2 G(\omega)$ for 0 GPa (black line) of Pmmm phase, 3 GPa (red line) and 10 GPa (blue line) of I4/mmm phase are shown in the 1st panel and the 3rd panel, respectively. The $F(\omega)$ and $\alpha^2 F(\omega)$ for 12 GPa (black line), 13 GPa (red line) of I4/mmm phase and 20 GPa (blue line) of C2/c are shown in the 2th panel and the 4th panel, respectively.

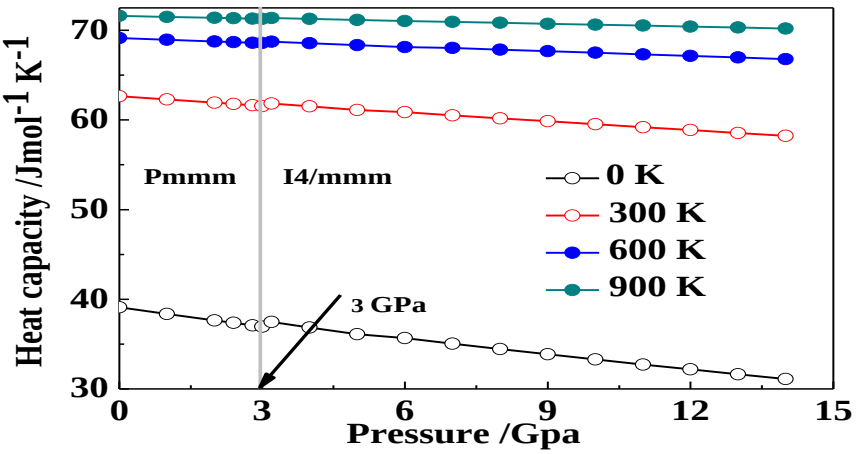

Fig. 5 Variation of heat capacity C_V with pressure at different temperature for CaN_2

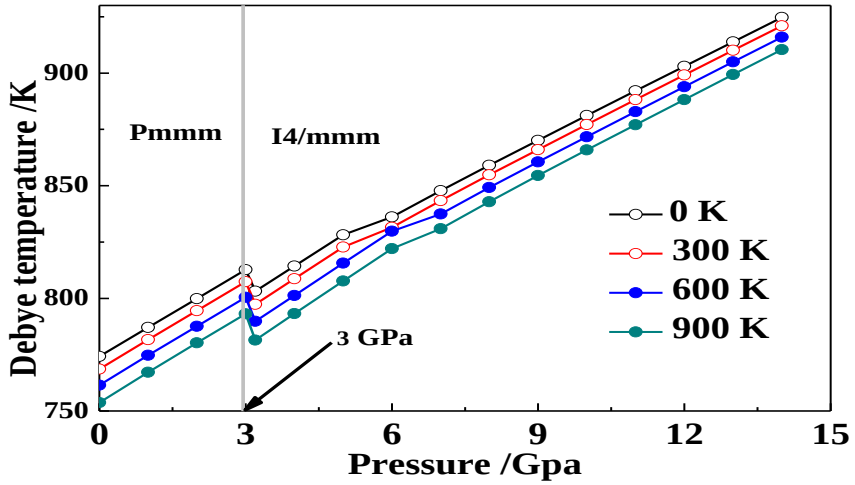

Fig.6 Variation of Debye temperature with pressure at different temperature for CaN_2

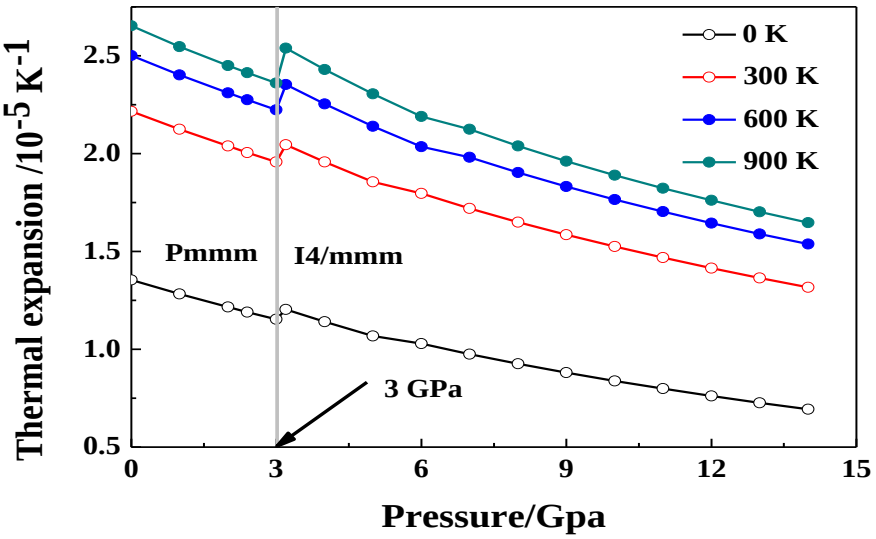

Fig. 7 Variation of thermal expansion α with pressure at different temperature for CaN_2

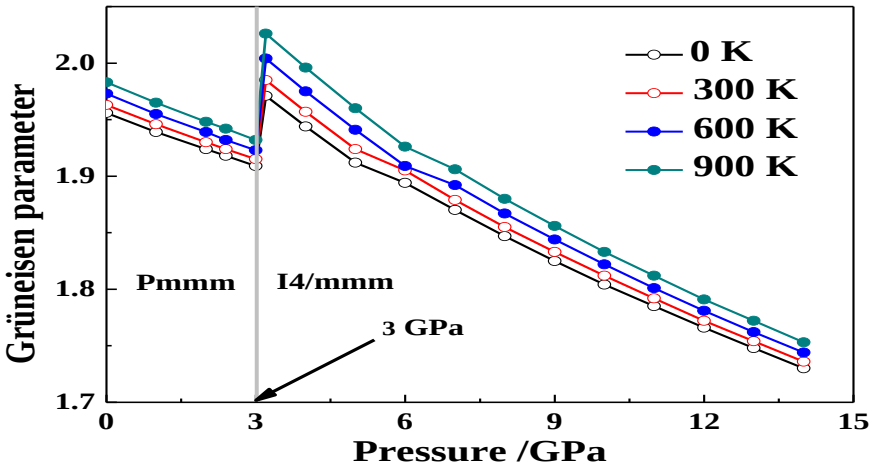

Fig. 8 Variation of Grüneisen parameter γ with pressure at different temperature for CaN_2

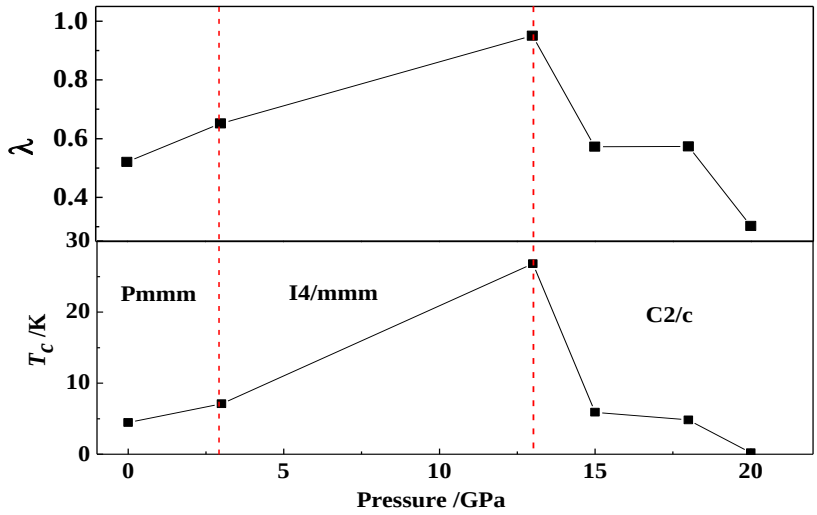

Fig. 9 T_c and λ as a function of pressure with $\mu^* = 0.1$

How to cite this article:

Zhang, QL., Zhang, FJ., Mu, SF., Zong, LG., Xu, TS. " Calculation of structure, phonon vibrational spectra, thermodynamic properties and superconductivity of calcium dinitride by First-principles " *J. Atoms and Molecules*, 8(5), 2018: 1181 - 1195

